Porous carbon nanotubes: Molecular absorption, transport, and separation

Irena Yzeiri, Niladri Patra, and Petr Král

Citation: The Journal of Chemical Physics **140**, 104704 (2014); doi: 10.1063/1.4867542
View online: http://dx.doi.org/10.1063/1.4867542
View Table of Contents: http://scitation.aip.org/content/aip/journal/jcp/140/10?ver=pdfcov
Published by the AIP Publishing

Porous carbon nanotubes: Molecular absorption, transport, and separation

Irena Yzeiri,[1] Niladri Patra,[1] and Petr Král[1,2,a)]
[1]*Department of Chemistry, University of Illinois at Chicago, Chicago, Illinois 60607, USA*
[2]*Department of Physics, University of Illinois at Chicago, Chicago, Illinois 60607, USA*

(Received 17 December 2013; accepted 22 February 2014; published online 11 March 2014)

We use classical molecular dynamics simulations to study nanofluidic properties of porous carbon nanotubes. We show that saturated water vapor condenses on the porous nanotubes, can be absorbed by them and transported in their interior. When these nanotubes are charged and placed in ionic solutions, they can selectively absorb ions in their interior and transport them. Porous carbon nanotubes can also be used as selective molecular sieves, as illustrated on a room temperature separation of benzene and ethanol. © *2014 AIP Publishing LLC*. [http://dx.doi.org/10.1063/1.4867542]

I. INTRODUCTION

Carbon nanotubes (CNTs) have many unique applications in nanofluidics, such as the possibility to drag molecules,[1–3] sense their flows,[4,5] separate molecules,[6–9] and desalinate solutions.[10,11] Nanofluidics can also be used to prepare novel graphene nanostructures.[12] Porous graphene (PG) with chemically functionalized nanopores has been introduced[13] and intensively tested for potential applications in molecular separation,[14–18] DNA sequencing,[19,20] and electronics.[21]

In principle, one could also introduce nanopores of tunable sizes, shapes, and chemistries in CNTs or "roll" porous graphene membrane into porous carbon nanotubes (PCNTs) with the goal to combine nanofluidic properties of PG and CNTs. Recently, such PCNTs were synthesized with nanopores of the diameters $d_p \approx 4$–10 nm, arranged either randomly[22] or in high density arrays.[23] Mechanical properties of these PCNTs depend on the pore sizes, symmetries, and densities.[24,25]

In this work, we examine by molecular dynamics (MD) simulations if PCNTs can inherit the nanofluidic properties of both PG and CNTs, which might result in nanochannels with *transversal* molecular selectivity and high *longitudinal* passage rates. To illustrate this idea, we study simultaneous molecular (transversal) absorption by PCNTs and (longitudinal) transport in their interiors. We also explore the possibility of ionic and molecular separation by arrays of charged and neutral PCNTs.

II. COMPUTATIONAL METHODS

We model all the processes by classical MD simulations with the NAMD package,[26] the CHARMM27 force field,[27] and the TIP3P model for water. The (non-bonding) van der Waals (vdW) coupling between *i*th and *j*th atoms is described by the Lennard-Jones potential,

$$V_{i,j} = \epsilon_{i,j}\,[(R_{min,i,j}/r_{i,j})^{12} - 2(R_{min,i,j}/r_{i,j})^{6}],$$
$$\epsilon_{i,j} = \sqrt{\epsilon_i\,\epsilon_j}, \quad R_{min,i,j} = \frac{1}{2}(R_{min,i} + R_{min,j}), \tag{1}$$

where we use $\epsilon_{\mathrm{O}} = -0.152$ kcal/mol, $R_{min,\mathrm{O}} = 3.4$ Å, and $\epsilon_{\mathrm{H}} = -0.046$ kcal/mol, $R_{min,\mathrm{H}} = 0.44$ Å (for TIP3P water), $\epsilon_{\mathrm{Na^+}} = -0.047$ kcal/mol, $R_{min,\mathrm{Na^+}} = 2.72$ Å, $\epsilon_{\mathrm{Cl^-}} = -0.150$ kcal/mol, $R_{min,\mathrm{Cl^-}} = 4.54$ Å. For carbon atoms of PCNTs, we use $\epsilon_{\mathrm{C}} = -0.07$ kcal/mol, $R_{min,\mathrm{C}} = 3.98$ Å. In our previous studies, we have obtained the vdW distance (3.4 Å) and energy (56 kcal/mol/nm^2) between two graphene layers[12] using the same L-J parameters for carbon atoms of graphene sheet. Here, we use the same L-J parameters for PCNTs carbon atoms. The non-bonded cut-off and the pair-list distance are 10 Å and 12 Å, respectively. We neglect the PCNT polarization and model the system with the Langevin dynamics,[28] the damping coefficient of 0.01 ps^{-1} (non-physical momentum dissipation[29]) and use the time step of 2 fs. The electrostatic interactions in the ionic systems are calculated using Particle mesh Ewald (PME).[30] PME is not used in the other systems that lack ions. For the condensation and separation of organic mixture studies, the carbon atoms of PCNT are neutral. In the ion separation studies, we homogeneously charge each carbon atom.

III. RESULTS AND DISCUSSION

A. Condensation and transport of water within PCNTs

Functionalized PCNTs might complement the spectrum of currently used desiccants, such as silica gel,[31] calcium sulfate and chloride,[32] and other molecular sieves.[33] In particular, PCNTs might be used to simultaneously absorb molecules from gas or liquid phases, and transport them away.

To test this possibility, we condense water vapor on the (28,28) PCNT (radius, $r = 1.9$ nm), as shown in Fig. 1. The hexagonal PCNT nanopores have a diameter of $d_p \approx 0.5$ nm, and they are hexagonally arranged with ≈0.7 nm separations. We place the (28,28) PCNT (25 nm long with fixed edge

a)Author to whom correspondence should be addressed. Electronic mail: pkral@uic.edu

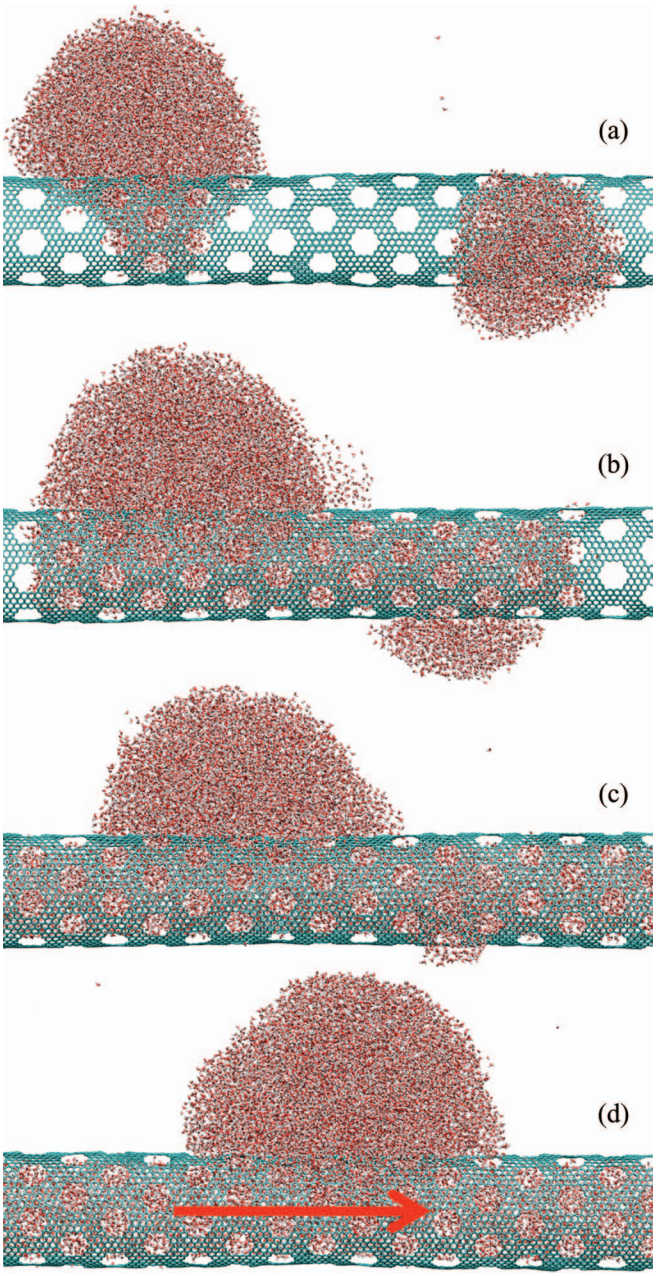

FIG. 1. Condensation of 40 000 water molecules from an oversaturated vapor into a (28,28) PCNT: (a) $t = 1$ ns, (b) 6 ns, and (c) 10 ns. At $t = 10$ ns, a pressure of $P \approx 156$ atm is applied to water at the left PCNT entrance, causing the absorbed water to flow through the tube with a speed of $v_w \approx 1.86$ nm/ns, as shown in (d) at $t = 14$ ns. The droplet adsorbed onto the PCNT moves with the flow with its own velocity of $v_d \approx 0.88$ nm/ns.

atoms; creates an infinite long PCNT without open ends) and 40 000 water molecules in a box ($25 \times 27 \times 25$ nm^3) with periodic conditions applied. Initially, the system is heated to $T = 600$ K to quickly vaporize the water and prepare the initial state of the system. Once it is slowly cooled to $T = 300$ K with a damping coefficient of 0.01 ps^{-1}, the vapor saturates, and condenses in the form of nanodroplets on the outer and inner PCNT surfaces. We obtain a two-phase (gas-liquid) system. Within $t \approx 1$ ns, droplets on both interior and exterior PCNT surfaces coalesce and interact through the nanopores, as seen in Fig. 1(a). The outer droplets are drawn by the inner droplets through the nanopores inside the PCNT, as seen in

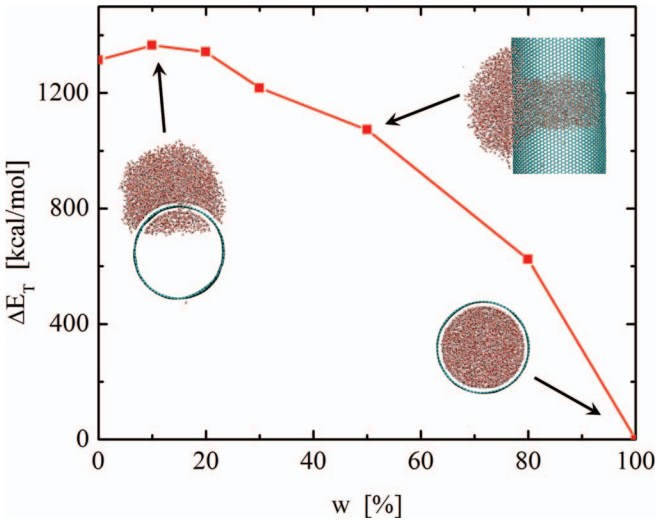

FIG. 2. The total change in energy when a water nanodroplet ($d_w \approx 6$ nm) enters inside a (40,40) PCNT through a single pore ($d_p \approx 1.5$ nm). Here, w is the relative amount of water inside the CNT.

Fig. 1(b) at $t \approx 6$ ns. Inside the PCNT, water has a lower energy due to additional vdW coupling to the walls.[34] At $t \approx 10$ ns, the PCNT is filled with water and the remaining water forms droplets condensed on its surface, as seen in Fig. 1(c).

Finally, in Fig. 1(d), we show that the water collected inside PCNT can be pumped through its interior by a small force of $f = 0.001$ kcal/mol/Å ($P \approx 156$ atm), applied on all the water molecules (each O and H atom) at the first 2 nm of the PCNT entrance. The water stays within the PCNTs and flows with an average velocity of $v_w \approx 1.86$ nm/ns. The internal water remains within the PCNT upon this established flow and drags the outer nanodroplet with a velocity of $v_d \approx 0.88$ nm/ns. Both, v_w and v_d depend on the applied force and the geometric details of the PCNT. If the applied force is large, the water molecules tend to leave the PCNT through the pores. We have simulated the water condensation and transport within different PCNTs (diameters of $d_T \approx 2$–6 nm, pore diameters of $d_p \approx 0.5$–1 nm, triangular pores) and observed qualitatively the same results with and without calculating the long range electrostatic interactions, using the PME method.[30]

In Fig. 2, we calculate the total energy of the system when a nanodroplet of a $d_w \approx 6$ nm diameter enters into a (40,40) CNT (radius, $r = 2.7$ nm) with one hexagonal pore ($d_p \approx 1.5$ nm). In order to obtain the potential energy in each step (Fig. 2), we equilibrate the system while keeping different amounts of water inside the tube by fixing (upon local equilibration) a thin dome-like layer of water molecules around the pore. Each step is simulated for $t \approx 4$ ns, and the total potential energy is calculated by averaging over last 500 frames of the trajectories using visual molecular dynamics (VMD) (CHARMM27 force field).[27,35] The simulations reveal that the energy barrier for the water droplet to enter the PCNT pore (≈10% of water inside) is $\Delta E_T \approx 50$ kcal/mol. The main contributions to this barrier come from the changing number of hydrogen bonds and varying vdW coupling energy between water and graphene during the droplet pas-

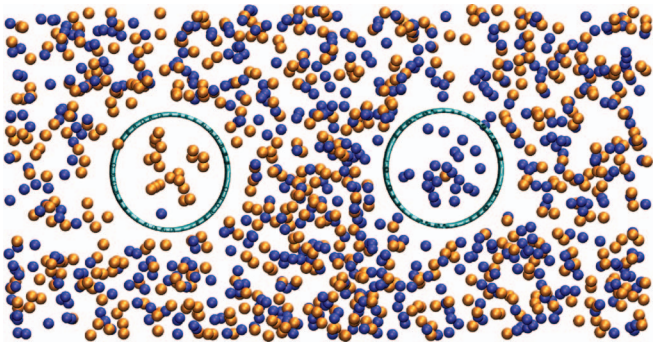

FIG. 3. Separation of Cl^- and Na^+ ions from the 0.2 M NaCl solution using oppositely charged (±0.02 e per carbon atom or ±50.8 e per tube) (20,20) PCNTs, 10 nm in length, at $T = 300$ K.

sage through the pore. Although water nanodroplets can enter partly filled PCNTs relatively easily, the results in Fig. 2 show that they experience a barrier when entering an empty PCNT. If the PCNT diameter is small enough, the droplet benefits from entering into the tube (vdW coupling), irrespective of the pore size. For a large nanotube, the droplet does not enter (entrance barrier is not reduced by additional vdW coupling to the PCNT interior), unless the diameter of the droplet is small enough to be comparable to that of the pore.

B. Exchange of ions using PCNTs

Charged CNTs can attract solvated ions onto their surfaces.[36–39] If PCNTs are charged and solvated in ionic solutions, they should attract ions, adsorb them into their interior, and potentially separate them from the solutions. This procedure might be useful in batteries,[40] supercapacitors,[41] and other ion-exchange devices. We briefly illustrate this idea on ion separation with two (20,20) PCNTs (radius, $r = 1.35$ nm) placed 4 nm apart in $C = 0.2$ M NaCl solution. The nanopores with a diameter of $d_p \approx 0.5$ nm are hexagonally arranged with ≈0.7 nm separations. We fix the atoms at the PCNT edges, oppositely and homogeneously charge the two PCNTs (±0.02e per carbon atom), and apply periodic boundary conditions to the system, so that ions only enter through the pores. The system is equilibrated in the NPT ensemble at a temperature of $T = 300$ K and a pressure of $P = 1$ atm.

In Fig. 3, we show the system after $t \approx 10$ ns of equilibration. We can see that oppositely charged ions enter into different PCNTs, but only ≈44% of the screening ions enter each PCNT (curvature). The remaining screening ions are within the Debye length, $\lambda_D = (\epsilon\, k_B\, T/e^2\, N_A\, 2\, C)^{1/2}$ ≈0.7 nm, of each PCNT. Since the PCNT internal diameter is $d_T \approx 2\,\lambda_D$, predominantly ions of the same charge are seen in the PCNT interiors, which is important for their selective separation. When we apply a small force of $f = 0.001$ kcal/mol/Å to the water molecules at the first 2 nm of the PCNT entrance ($P \approx 110$ atm), the charged ionic solution inside each tube flows with a speed of $v_i \approx 0.81$ nm/ns. In principle, this allows for the replacement of the ions in the system. The selectivity, speed, and efficiency of this process can be tuned by the type of PCNTs and the solution used. Additional changes can be expected in the presence of functionalized pores. The system behavior can be slightly different when a polarized force field is used.[13] For large pores, these effects might be less important.

C. Separation of organic mixtures using PCNTs

Next, we examine if neutral PCNTs could be used in the separation of molecules passing through their walls. Pristine CNTs with relatively small diameters ($d_t \approx 2$ nm) can separate ethanol from ethanol-water solution with a very high efficiency and selectivity.[42,43] However, the requirement of narrow CNTs is quite strong. Therefore, it would be very interesting if PCNTs with tunable pore sizes could separate such molecular mixtures. Different coupling between the molecules and potentially functionalized PCNTs might help in the separation process. We are particularly interested in separating organic compounds with similar boiling points, $\Delta T_b \approx 0$, which is hard to do by fractional distillation or alike methods.

Here, we test if plain (no functionalization) PCNTs could separate a mixture of benzene and ethanol, with $\Delta T_b \approx 2\,^\circ$C ($T_{benzene} = 80.1\,^\circ$C, $T_{ethanol} = 78.4\,^\circ$C). In this work, we evaluate the separation efficiency depending on the PCNT diameter, temperature, and mixture composition. First, we simulate the molecular separation by (20,20), (28,28), and (40,40) PCNTs with hexagonal nanopores having a diameter of $d_p \approx 1$ nm, hexagonally arranged with ≈0.7 nm separations. The PCNTs are immersed in the (1:1) benzene-ethanol binary mixture in a $16 \times 11 \times 10$ nm^3 box with periodic boundary conditions applied. We simulate the systems in the NPT ensemble at $T = 300$ K and $P = 1$ atm.

Figure 4 (top) shows the equilibrated percentual radial distribution of benzene in these PCNTs. We calculate the distributions in cylindrical shells oriented along the PCNT axis and radially separated by 0.2 nm. One can clearly see that the molecular separation is possible in narrow PCNTs. The concentration of benzene inside the (20,20) PCNT is ≈98%, while it is only ≈62% inside the (40,40) PCNT. Therefore, PCNTs with smaller radii could separate molecules more efficiently, since all the molecules inside the tube either couple directly to the walls or they couple to the first layer of benzene adsorbed at the walls.

In the inset of Fig. 4 (middle), we show the distribution obtained in the smallest (20,20) PCNT after $t = 20$ ns of simulations. We can clearly see that the PCNT interior is predominantly filled by benzene (dark) and so is its external surface. It is because benzene has a stronger vdW coupling to PCNT than ethanol; we have calculated by VMD the average vdW binding energy density for CNT-benzene (0.75 kcal/mol/atom) and CNT-ethanol (0.60 kcal/mol/atom).[44]

In Fig. 4 (middle), we study the effect of temperature on the separation efficiency in the (20,20) PCNT. We can see that as the temperature is increased from $T = 300$ K to $T = 325$ K and $T = 340$ K, the separation efficiency (average benzene concentration) drops from ≈98% to ≈90% and ≈80%, respectively. This is caused by the fact that thermal fluctuations tend to break the stronger benzene-nanotube vdW bonding, making the PCNT entrance for both types of molecules equally likely. In this work, we do not pay a

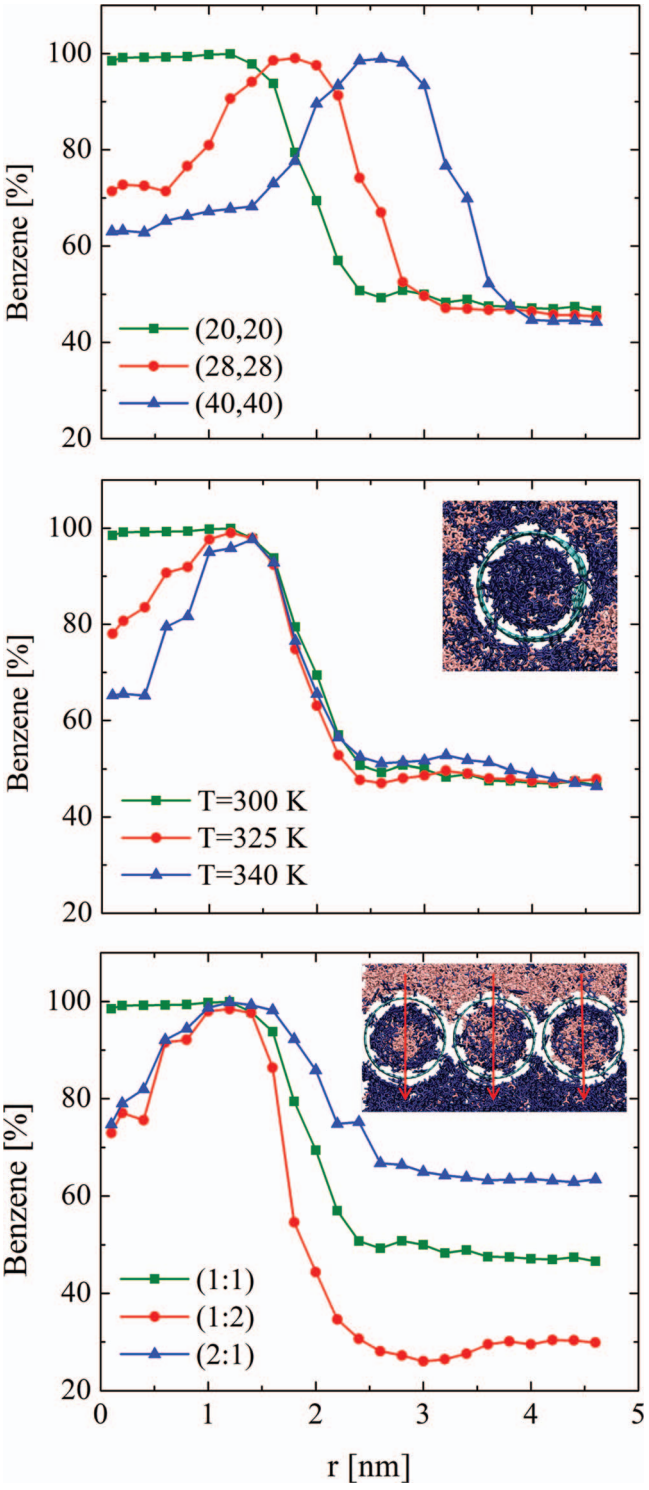

FIG. 4. (Top) Separation of the (1:1) benzene-ethanol mixture at $T = 300$ K with the (20,20), (28,28), and (40,40) PCNTs having $d_p \approx 1$ nm nanopores. (Middle) The same in the (20,20) PCNT at different temperatures. (Inset) The distribution of benzene (dark) and ethanol inside (20,20) PCNT after $t = 20$ ns of simulations. (Bottom) Separation of the (1:1), (1:2), (2:1) benzene-ethanol mixtures in the (20,20) PCNT at $T = 300$ K. (Inset) Separation of benzene from the benzene-ethanol (1:1) binary mixture at $T = 300$ K using a (20,20) PCNT membrane. Vertical arrows show direction of flow.

particular attention to the pore sizes and their chemistry, since the pores are large. Therefore, the molecular separation is largely influenced by the coupling of the molecules to the PCNT wall.

Finally, we investigate how the molecular separation efficiency depends on the composition of the binary mixture. We simulate the separation of the (1:1), (1:2), and (2:1) benzene-ethanol mixtures in the (20,20) PCNT. In Fig. 4 (bottom), we observe that the separation is very efficient under the (1:1) conditions. However, as we increase the concentration of either component to (1:2) or (2:1), the separation efficiency decreases. This was expected for the (1:2) benzene-ethanol composition, but it is a rather unexpected result for the (2:1) composition. During a closer inspection of our simulations, we observe clusters of ethanol forming under the (1:2) and (2:1) benzene-ethanol compositions, which could be caused by a limited miscibility of benzene and ethanol. In realistic systems with organic molecules, the separation ability might be more limited. The molecular phases can also be modified in the PCNT interior.

In the inset of Fig. 4 (bottom), we also illustrate how PCNTs could be practically used in the separation of organic mixtures. We simulate the molecular passage through a membrane formed of adjacent parallel (fixed) (20,20) PCNTs with hexagonally arranged (0.7 nm apart) pores ($d_p \approx 0.5$ nm). The (1:1) benzene-ethanol mixture is placed on the top of the PCNT membrane. A layer of dummy atoms placed 5 nm below the membrane prevents mixing of the solutions above and below the membrane (periodic system and NVT ensemble). The solution above the PCNT membrane is pressurized by applying on all the solution atoms (5 nm above the membrane) a small force of $f = 5$ cal/mol/Å oriented normal to the membrane. As a result, the solution flows down, but predominantly benzene molecules are passing through the membrane, thus separating the binary mixture. After $t = 10$ ns, the molar ratio of benzene and ethanol below the PCNT membrane is 96:4. The separation efficiency may be improved by the use of multilayer membranes. In reality, the situation can be much more complex which could not be studied by classical MD methods. The observed phenomena might be quantitatively modified if more precise force fields are used, which are also matched to the experiments.

IV. CONCLUSIONS

We have demonstrated that PCNTs could be used in selective molecular absorption, transport, and separation. We have shown that saturated water vapor can be absorbed on and pumped out by PCNTs, which might be used in active desiccation. Different types of ions can also be separated from ionic solutions and pumped away through charged PCNTs, which might be used in batteries and supercapacitors. PCNTs might also serve as molecular sieves, where molecules can be efficiently separated based on their coupling to PCNTs. Therefore, porous nanotubes made from atomic and molecular components can form an important class of materials with a broad range of applications.

ACKNOWLEDGMENTS

This work was supported by the NSF Grant No. CBET-0932812. Niladri Patra acknowledges support from UIC Harbert E. Paaren Academic Year Research Fellowship. The

presented calculations have been partly performed on the NERSC and NCSA supercomputer networks.

[1]P. Král and D. Tománek, Phys. Rev. Lett. **82**, 5373 (1999).
[2]B. C. Regan, S. Aloni, R. O. Ritchie, U. Dahmen, and A. Zettl, Nature (London) **428**, 924 (2004).
[3]P. Xiu, B. Zhou, W. Qi, H. Lu, Y. Tu, and H. Fang, J. Am. Chem. Soc. **131**, 2840 (2009).
[4]P. Král and M. Shapiro, Phys. Rev. Lett. **86**, 131 (2001).
[5]S. Ghosh, S. K. Sood, and N. Kumar, Science **299**, 1042 (2003).
[6]G. Stan, J. Low Temp. Phys. **157**, 374 (2009).
[7]A. Gaurav and S. I. Sandler, J. Chem. Phys. **123**, 044705 (2005).
[8]S. Blankenburg, M. Bieri, R. Fasel, K. Müllen, C. A. Pignedoli, and D. Passerone, Small **6**, 2226 (2010).
[9]J. Lee and N. R. Aluru, Appl. Phys. Lett. **96**, 133108 (2010).
[10]B. Corry, J. Phys. Chem. B **112**, 1427 (2008).
[11]A. Noy, H. G. Park, F. Fornasiero, C. P. Holt, C. P. Grigoropoulos, and O. Bakajin, Nano Today **2**, 22 (2007).
[12]N. Patra, B. Wang, and P. Král, Nano Lett. **9**, 3766 (2009).
[13]K. Sint, B. Wang, and P. Král, J. Am. Chem. Soc. **130**, 16448 (2008).
[14]A. W. Hauser and P. Schwerdtfeger, J. Phys. Chem. Lett. **3**, 209 (2012).
[15]R. R. Nair, H. A. Wu, P. N. Jayaram, I. Grigorieva, and A. K. Geim, Science **335**, 442 (2012).
[16]S. P. Koenig, L. Wang, J. Pellegrino, and J. S. Bunch, Nat. Nanotechnol. **7**, 728 (2012).
[17]D. Jiang, V. R. Cooper, and S. Dai, Nano Lett. **9**, 4019 (2009).
[18]L. L. Zhang, X. Zhao, M. D. Stoller, Y. Zhu, H. Ji, S. Murali, Y. Wu, S. Perales, B. Clevenger, and R. S. Ruoff, Nano Lett. **12**, 1806 (2012).
[19]S. Garaj, W. Hubbard, A. Reina, J. Kong, D. Branton, and J. A. Golovchenko, Nature (London) **467**, 190 (2010).
[20]T. Nelson, B. Zhang, and O. V. Prezhdo, Nano Lett. **10**, 3237 (2010).
[21]A. Baskin and P. Král, Sci. Rep. **1**, 36 (2011).
[22]M. Kim, K. Sohn, J. Kim, and T. Hyeon, Chem. Commun. **2003**, 652.
[23]A. T. Rodrigues, M. Chen, Z. Chen, C. J. Brinker, and H. Fan, J. Am. Chem. Soc. **128**, 9276 (2006).
[24]D. D. T. K. Kulathunga, K. K. Ang, and J. N. Reddy, J. Phys.: Condens. Matter **22**, 345301 (2010).
[25]Y. Hirai, S. Nishimaki, H. Mori, Y. Kimoto, S. Akita, Y. Nakayama, and Y. Tanaka, Jpn. J. Appl. Phys. **42**, 4120 (2003).
[26]J. C. Phillips, R. Braun, W. Wang, J. Gumbart, E. Tajkhorshid, E. Villa, C. Chipot, R. D. Skeel, L. Kale, and K. J. Schulten, J. Comput. Chem. **26**, 1781 (2005).
[27]A. D. MacKerell, Jr., D. Bashford, M. Bellott, R. L. Dunbrack, Jr., J. D. Evanseck, M. J. Field, S. Fischer, J. Gao, H. Guo, S. Ha *et al.*, J. Phys. Chem. B **102**, 3586 (1998).
[28]J. Servantie and P. Gaspard, Phys. Rev. Lett. **91**, 185503 (2003).
[29]S. E. Feller, Y. H. Zhang, R. W. Pastor, and B. Brooks, J. Chem. Phys. **103**, 4613 (1995).
[30]T. Darden, D. York, and L. Pederson, J. Chem. Phys. **98**, 10089 (1993).
[31]H. Hata, S. Saeki, T. Kimura, Y. Sugahara, and K. Kuroda, Chem. Mater. **11**, 1110 (1999).
[32]R. D. Burfield, K. Lee, and H. R. Smithers, J. Org. Chem. **42**, 3060 (1977).
[33]M. E. Davis and R. F. Lobo, Chem. Mater. **4**, 756 (1992).
[34]A. Kalra, S. Garde, and G. Hummer, Proc. Natl. Acad. Sci. U.S.A. **100**, 10175 (2003).
[35]W. Humphrey, A. Dalke, and K. Schulten, J. Mol. Graphics **14**, 33 (1996).
[36]T. A. Beu, J. Chem. Phys. **132**, 164513 (2010).
[37]F. Fornasiero, H. G. Park, J. K. Holt, M. Stadermann, C. P. Grigoropoulos, A. Noy, and O. Bakajin, Proc. Natl. Acad. Sci. U.S.A. **105**, 17250 (2008).
[38]S. Banerjee, S. Murad, and I. K. Puri, Chem. Phys. Lett. **434**, 292 (2007).
[39]J. H. Park, S. B. Sinnott, and N. R. Aluru, Nanotechnology **17**, 895 (2006).
[40]S. W. Lee, N. Yabuuchi, B. M. Gallant, S. Chen, B. Kim, P. T. Hammond, and Y. Shao-Horn, Nat. Nanotechnol. **5**, 531 (2010).
[41]H. Pan, J. Li, and Y. P. Feng, Nanoscale Res. Lett. **5**, 654 (2010).
[42]W. Zhao, B. Shang, S. Du, L. Yuan, and J. Yang, J. Chem. Phys. **137**, 034501 (2012).
[43]Z. Mao and B. Sinnott, J. Phys. Chem. B **105**, 6916 (2001).
[44]The CNT-benzene (or CNT-ethanol) binding energies are calculated as the difference of the total vdW energy of the system, when the system components are at the normal binding distance, and when they are separated by 5 nm. Averaging of the energies is done over 200 consecutive frames of the simulation trajectory, with a 1 ps time interval. The binding energy density (kcal/mol/atom) of CNT-benzene is obtained from dividing the average binding energy by the number of atoms of benzene molecules. Similarly, CNT-ethanol binding energy density is calculated.